CHEMISTRY
A EUROPEAN JOURNAL

DOI: 10.1002/chem.201000046

Transition States and Origins of 1,4-Asymmetric Induction in Alkylations of 2,2,6-Trialkylpiperidine Enamines

Joann M. Um,[a] Naeem S. Kaka,[b] David M. Hodgson,*[b] and K. N. Houk*[a]

Abstract: The asymmetric *C*-alkylation of chiral enamines derived from terminal epoxides and lithium 2,2,6-trialkylpiperidides has previously been shown to provide α-alkylated aldehydes by intermolecular nucleophilic substitution in good levels of asymmetric induction. We now report a computational study of the origins of asymmetric induction in these reactions. Computational modeling with density functional theory (B3LYP/6-31G(d)) agrees closely with the experimental observations. This stereoselectivity is attributed to a preferential conformation of the enamine and the piperidine ring that places the C-6 alkyl substituent in an axial position due to $A^{1,3}$ strain. Preferential attack occurs away from the axial group, for steric reasons. The effects of changing the C-6 substituent from methyl to isopropyl were studied, and twist transition states were found to contribute significantly in the latter alkylations.

Keywords: aldehydes · alkylation · asymmetric synthesis · density functional calculations · transition states

Introduction

Direct generation of enantioenriched mono-α-alkylated aldehydes by C–C bond formation involving intermolecular nucleophilic substitution has been a long-standing interest in synthesis.[1] While significant progress has been made in the organocatalytic asymmetric enamine-based α-functionalization of aldehydes, including intramolecular alkylation[2] and the use of (radical-stabilized) α-bromocarbonyl compounds as electrophiles,[3] direct alkylation with simple alkyl halides has remained problematic. We recently reported the asymmetric synthesis of α-alkylated aldehydes using terminal epoxide-derived chiral enamines (Scheme 1).[4] In that earlier work, we examined the enamine derived from 1,2-epoxyhexane **1** ($R^1 = C_4H_9$) and lithium 2,2,6-trimethylpiperidide **2** ($R^2 = Me$). We observed that the latter was bulky enough to form the corresponding methyl enamine **3a** in good yield, avoiding potentially competing allylic alcohol/amino alcohol formation. The enamine underwent effective *C*-alkylation to generate α-alkylated aldehydes **4**. By contrast, the enamine derived from lithium 2,2,6,6-tetramethylpiperidine (LTMP) was slow to react, affording the α-methylated aldehyde in only 30% yield.[5]

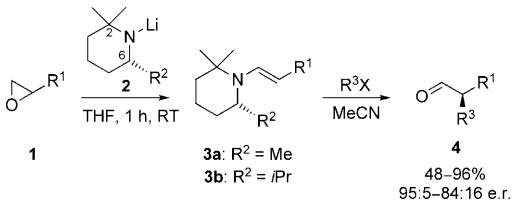

Scheme 1. Asymmetric synthesis of α-alkylated aldehydes from terminal epoxide-derived chiral enamines.[4]

Our original hypothesis was that the single C-6 piperidinyl substituent (R^2) would reside axially in the corresponding methyl enamine **3a**, not only to minimize $A^{1,3}$ strain, but also to allow effective *N* lone pair–π* interaction, which is essential for enamine reactivity (Figure 1, conformer **6**).[6] The conformation in which the R^2 group lies in an equatorial position (**7**) would lead to $A^{1,3}$ strain.

A range of electrophiles proved viable with racemic methyl enamine **3a**, including Michael acceptors, activated organohalides and unactivated alkyl iodides (methyl-, ethyl-, decyl-, and isopropyl iodide).[4] When methyl enamine **3a**

[a] J. M. Um, Prof. K. N. Houk
Department of Chemistry and Biochemistry, UCLA
Los Angeles, CA 90095-1569 (USA)
Fax: (+1) 310-206-1843
E-mail: houk@chem.ucla.edu

[b] Dr. N. S. Kaka, Prof. D. M. Hodgson
Department of Chemistry, Chemistry Research Laboratory
University of Oxford, Mansfield Road, Oxford, OX1 3TA (UK)
Fax: (+44) 1865-285002
E-mail: david.hodgson@chem.ox.ac.uk

Supporting information for this article is available on the WWW under http://dx.doi.org/10.1002/chem.201000046.

WILEY InterScience DISCOVER SOMETHING GREAT
© 2010 Wiley-VCH Verlag GmbH & Co. KGaA, Weinheim

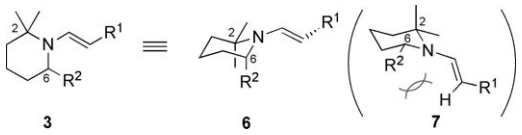

Figure 1. Enamine **3** conformers.

was used as a single enantiomer in alkylations with ethyl iodide and allyl bromide, the corresponding α-alkylated aldehydes were formed in satisfactory e.r. values (88:12 e.r. and 84:16 e.r., respectively), with the sense of asymmetric induction as shown in Scheme 1.[4] Work-up after enamine alkylation using AcOD/NaOAc/D_2O showed no D incorporation, indicating that no loss of enantiointegrity occurred during hydrolysis.[4] With the aim of improving the enantiomeric ratios obtained with enamine **3a**, a lithium amide with an isopropyl group as a sterically more demanding substituent at C-6 was subsequently examined. Isopropyl enamine **3b** reacted with activated organohalides (allyl-, benzyl- and propargyl bromides) and importantly, also with simple alkyl iodides (MeI and EtI) providing the first highly enantioenriched α-alkylated aldehydes via intermolecular nucleophilic substitution (Scheme 1).[4]

We now provide computational studies of these enamine alkylations using ethyl iodide and allyl bromide as representative electrophiles, and give a more quantitative description of the origins of stereoselectivity. To the best of our knowledge, this report is the only quantum mechanical investigation of alkylation reactions by piperidine-derived enamines.[7] The C_4H_9 group (R^1) on the enamine/iminium ion was modeled as CH_3. The labels of model enamines are starred. Units of energy are expressed in kJ mol^{-1}. *anti* and *syn* refer to the relationship between the double bond and the N–C bond bearing the geminal methyl groups (Figure 2).

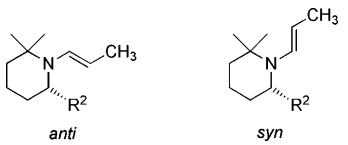

Figure 2. *anti*/*syn* Relationship.

Results and Discussion

Methyl enamine 3a* ground-state conformations: We postulated that the C-6 methyl substituent of methyl enamine **3a** would reside in an axial position to avoid $A^{1,3}$ strain and to allow favorable orbital interaction between the *N* lone pair and the alkene π* orbital. Indeed, the ^{1}H NMR chemical shift difference between the two olefinic protons of enamine **3a** is 1.41 ppm, indicative of traditional enamine-like character.[6] Conformational analysis of enamine **3a*** with B3LYP/6-31G(d) provided further support for this analysis. The lowest energy conformer of enamine **3a*** has an axial C-6 methyl group and effective enamine conjugation (**GS1**, *anti*-chair, Figure 3). Conformer **GS1** was found to be 8.5 kJ mol^{-1} lower in energy than the equatorial C-6 methyl conformer (**GS2**, *anti*-chair); at 25 °C, this corresponds to a 97:3 equilibrium ratio. In the latter conformation (**GS2**), the unfavorable repulsion between the equatorial C-6-Me and the distal H (NCH=C*H*) on the alkene causes the *N* lone pair–alkene π* interaction to decrease. The N–C7 and C7–C8 bond lengths of **GS2** are 1.41 and 1.34 Å, indicating a smaller degree of conjugation than **GS1**, where the corresponding distances are 1.39 and 1.35 Å, respectively.

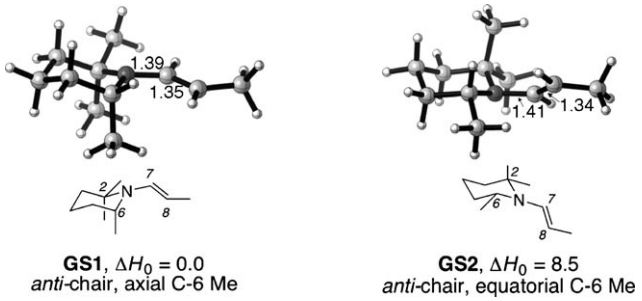

Figure 3. Ground-state conformations and relative enthalpies of methyl enamine **3a***.

Higher energy conformers of **3a*** are shown in Figure 4. The *anti*-twist conformation (**GS3**, axial C-6 methyl) is 10.0 kJ mol^{-1} less stable than **GS1** and the former does not suffer from 1,3-diaxial interaction between *cis* methyl groups present in chair conformer **GS1**; however, torsional strain in **GS3** outweighs the beneficial factors of diaxial strain relief. The *anti*-twist-boat conformation **GS4** is 2.2 kJ mol^{-1} higher in energy than **GS3**, due to a 2-Me, 4-H 1,3-diaxial interaction. Finally, *syn*-chair conformer **GS5** (equatorial C-6 methyl) is 17.3 kJ mol^{-1} higher in energy than **GS1** due to repulsion between the distal H (NCH=C*H*) of the alkene and the C-2 axial methyl group. Due to the significantly higher energies of **GS2**–**GS5** relative to **GS1**, **GS2**–**GS5** should not be present in any significant amount at equilibrium.

Transition structures for alkylation of methyl enamine 3a*: Methyl enamine **3a** undergoes alkylation with ethyl iodide and allyl bromide in 88:12 and 84:16 e.r., furnishing aldehydes (*R*)-**4a** and (*S*)-**4b**, respectively (Scheme 2).[4]

The lowest energy transition states involve attack of ethyl iodide on the *Re* face of the *anti*-chair and *anti*-twist enamines (**TS1** and **TS2**, Figure 5). The *anti*-twist transition structure **TS2** (originating from **GS3**) is 5.5 kJ mol^{-1} higher in energy than **TS1**, which originates from **GS1**. The transition structure that would originate from **GS2** converges to **TS2**. These transition structures lead to the major iminium diastereomer and to the observed major aldehyde enantiomer after hydrolysis. The deviation of the iodide from linearity with respect to the forming and breaking bonds is due to the fact that the iodide leans towards the piperidine hydrogens for electrostatic stabilization.[8] Compared to the transi-

 © 2010 Wiley-VCH Verlag GmbH & Co. KGaA, Weinheim

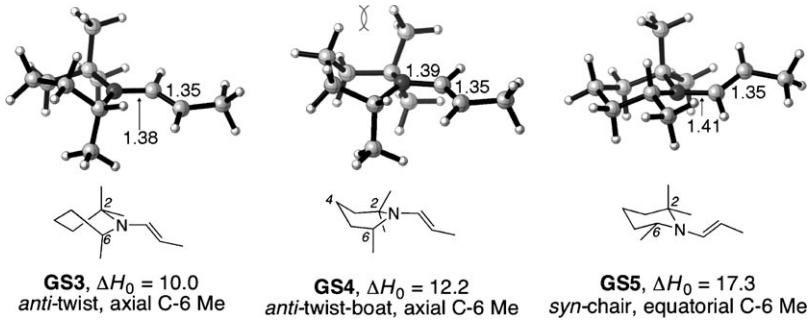

Figure 4. Higher energy ground-state conformations and relative enthalpies of methyl enamine **3a***.

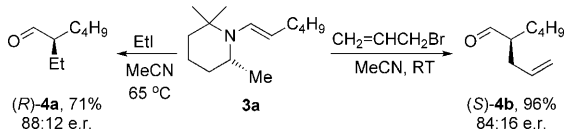

Scheme 2. Methyl enamine **3a** alkylation with ethyl iodide and allyl bromide.[4]

tion structures optimized in the gas phase, the angles between the forming C–C bond and halide of the solution-phase transition structures are more linear by an average of 9°, and the shortest distances between the halide and a piperidine hydrogen of the solvent-optimized transition structures are 0.68 Å longer.

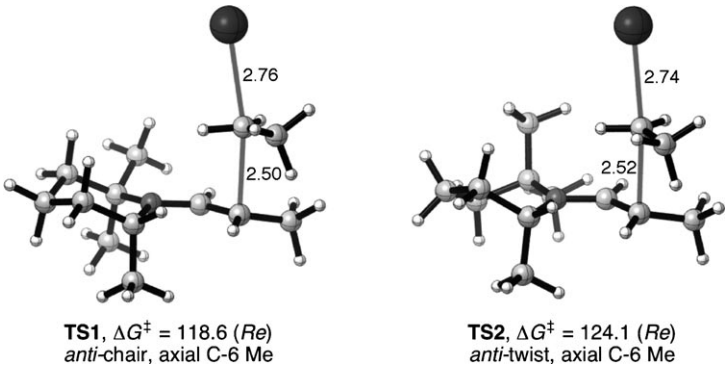

Figure 5. *Re*-face transition states for alkylation of methyl enamine **3a*** with ethyl iodide.

Ethyl iodide alkylation of enamine **3a*** via the *Si* face leads to the minor iminium diastereomer; the transition states **TS3** (*anti*-chair, axial C-6 methyl, Figure 6) and **TS4** (*anti*-twist, axial C-6 methyl, Figure 6) for this process are 3.6 and 10.7 kJ mol^{-1} higher in energy than **TS1**, respectively. This results in an overall calculated e.r. of 79:21, which corresponds to an apparent $\Delta\Delta G^{\ddagger}$ of 3.8 kJ mol^{-1} at 65 °C. The calculated selectivity is in good agreement with the experimental e.r. of 88:12 ($\Delta\Delta G^{\ddagger} = 5.6$ kJ mol^{-1} at 65 °C). The selectivity for *Re*-face attack may be attributed to unfavorable interaction between the electrophile and axial C-6 methyl group in the *Si*-face transition state. If one views the two axial methyl groups of **GS1** as part of a six-membered ring (dashed in **8**, Figure 7), then facial selectivity should disappear. In other words, the C-6–H and N–C-7 bonds would be eclipsed, and the nucleophilic carbon (C-8) would be equidistant to H_a and H_b. In reality, in the chair-like transition states, the alkene moiety is not equidistant with H_a and H_b, but

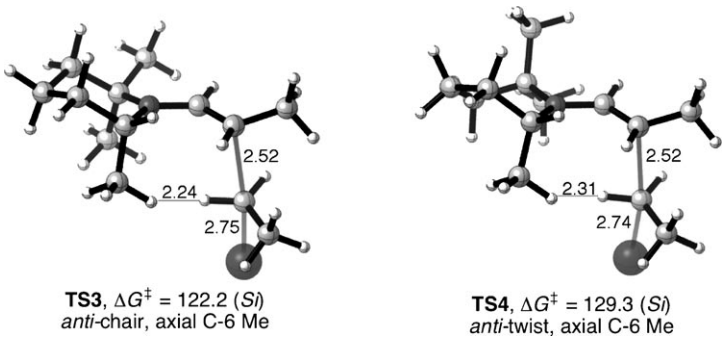

Figure 6. *Si*-face alkylation transition states for the reaction of methyl enamine **3a*** with ethyl iodide.

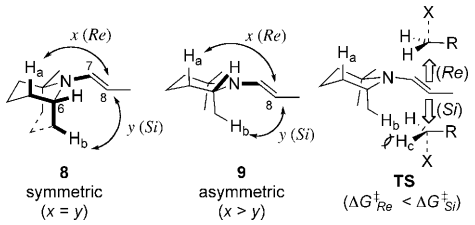

Figure 7. Origin of asymmetric induction for methyl enamine **3a** alkylations.

rather lies closer to H_b (see **9**, and compare C-8–H_a and C-8–H_b distances in Table 1), since the six-membered ring is flattened as compared to the ideal staggered arrangement,[9]

Table 1. Transition state C–H and H–H distances for methyl enamine **3a*** alkylations.

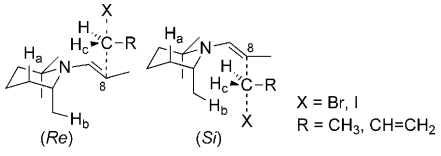

Entry	TS	C8–H_a [Å]	C8–H_b [Å]	H_c–H_a [Å]	H_c–H_b [Å]
1	**1** (*Re*)	4.51	2.93	3.22	–
2	**3** (*Si*)	4.46	3.04	–	2.24
3	**5** (*Re*)	4.49	2.97	3.07	–
4	**7** (*Si*)	4.45	3.05	–	2.19

© 2010 Wiley-VCH Verlag GmbH & Co. KGaA, Weinheim

due to a combination of developing *N* lone pair–π* interaction and splaying of the axial methyl groups to reduce 1,3-diaxial interaction. Attack of the electrophile from the *Si* face (see **TS**, Figure 7) results in unfavorable interaction between a hydrogen on the electrophilic carbon (H_c) and H_b (Table 1, compare H_c–H_a and H_c–H_b distances). The distances between these hydrogens lie within the H–H van der Waals radius of 2.4 Å and result in the observed stereoselectivity.

The lowest energy major and minor transition structures for the allylation of enamine **3a*** with allyl bromide are shown in Figure 8.[10] As in the case with ethyl iodide, *Re*-face allylation is preferred, with a calculated e.r. of 91:9 ($\Delta\Delta G^{\ddagger} = 5.7\ kJ\,mol^{-1}$ at 25 °C). This calculated value is again in good agreement with that observed experimentally (84:16 e.r., $\Delta\Delta G^{\ddagger} = 4.1\ kJ\,mol^{-1}$ at room temperature).

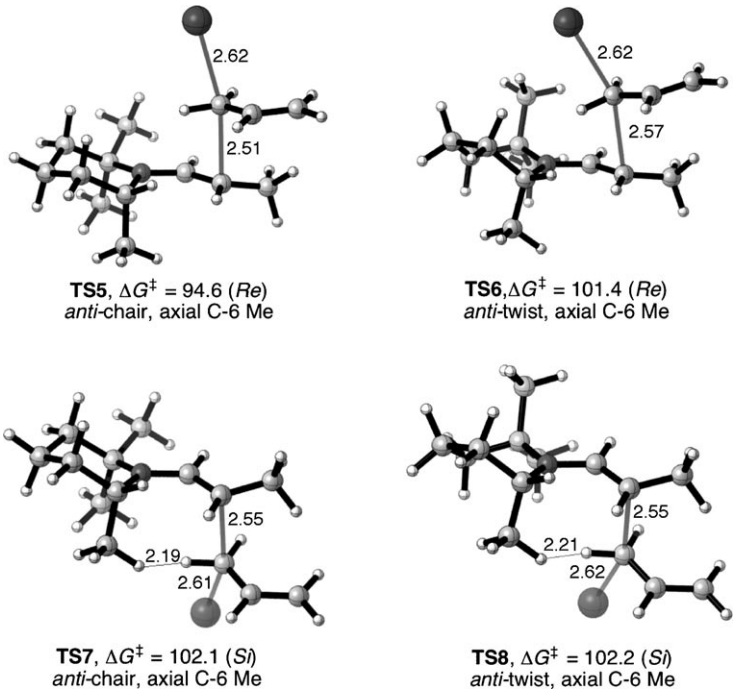

Figure 8. *Re*- and *Si*-face alkylation transition states for reaction of methyl enamine **3a*** with allyl bromide.

While the experimental stereoselectivity for alkylation of **3a** decreases in going from ethyl iodide (88:12) to allyl bromide (84:16), our calculations predict an increase in the selectivity from ethyl iodide (79:21) to allyl bromide (91:9). This high calculated selectivity can be explained by a large hydrogen–bromide stabilization in the favored (*Re*) transition states **TS5** and **TS6**, in which the stabilizing H–Br distances are up to 1.42 Å shorter than those of the corresponding ethyl iodide transition structures (**TS1** and **TS2**).[8] This difference can potentially be explained by the higher reactivity and more dissociative nature of the allyl halides compared with the ethyl halides due to the greater stability of allyl cations. The average C–I distance in **TS1–4** is 2.75 Å (131 % of a fully formed 2.1 Å C–I bond). In comparison, the average C–Br distance in **TS5–8** is 2.61 Å (137 % of a fully formed 1.9 Å C–Br bond). Likewise, the forming C–C bonds of **TS5–8** are longer than those of **TS1–4** by an average of 0.04 Å. The bromides thus lean towards the piperidine hydrogens for stabilization more than the iodides. It is likely that explicit solvation will further reduce the non-linearity of the allyl halide transition structures.

Isopropyl enamine 3b* ground-state conformations: The encouraging e.r. values obtained using methyl enamine **3a** led us to investigate the isopropyl enamine **3b**, with a bulkier alkyl group α-to the nitrogen. We initially anticipated that for $R^2 = i$Pr, the isopropyl group would reside axially (conformer **6** ($R^2 = i$Pr), Figure 1) and provide greater hindrance for electrophilic approach from the *Si* (lower) face. The isopropyl enamine **3b**, however, displays a ^{1}H NMR chemical shift difference between the two olefinic protons of only 0.33 ppm, indicative that the *N* lone pair and alkene π orbital are not aligned.[6] This suggests that the isopropyl group is in an equatorial position (**7**, Figure 1). A DFT conformational analysis of enamine **3b*** confirmed that the lowest energy conformer is one where the C-6 isopropyl group occupies an equatorial position; this in turn causes the *N* lone pair and alkene π orbital to become orthogonal to each other (**GS6**, Figure 9). The conformer with an axial isopropyl group (**GS7**) was found to be 5.4 kJ mol^{-1} higher in energy than **GS6**.

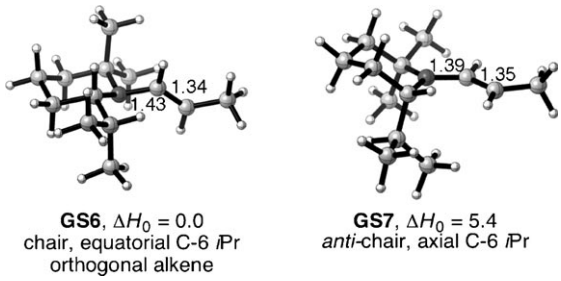

Figure 9. Ground-state conformations and relative enthalpies of isopropyl enamine **3b***.

Furthermore, an *anti*-chair conformer (**GS8**, Figure 10) with the C-6 isopropyl group equatorial, but with interaction between the *N* lone pair and alkene π orbital, was calculated to be 6.7 kJ mol^{-1} higher in energy than **GS6**. An *anti*-twist conformer (**GS9**, axial C-6 isopropyl) was also calculated to be 4.7 kJ mol^{-1} higher in energy than **GS6**. The lower energy of **GS9** compared to **GS7** can be attributed to the absence of an unfavorable 1,3-diaxial interaction between a C-2-Me and the C-6-*i*Pr in the former.

It can be concluded that the energy gained on enamine stabilization (*N* lone pair–alkene π* interaction) outweighs unfavorable 1,3-diaxial interaction between the axial C-6 and C-2 methyl groups for methyl enamine **3a*** (**GS1**, Figure 3); however, the opposite is true for isopropyl en-

 © 2010 Wiley-VCH Verlag GmbH & Co. KGaA, Weinheim

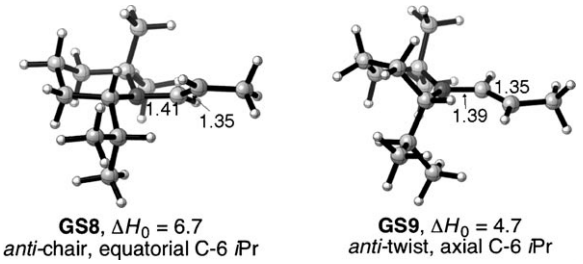

Figure 10. Additional ground-state conformations and relative enthalpies of isopropyl enamine **3b***.

amine **3b***, where unfavorable 1,3-diaxial interaction between the axial C-6 isopropyl group and axial C-2 methyl group outweigh the energy gained by enamine conjugation.

To support our analysis of the conformational preferences of enamines **3a** and **3b**, we calculated the ^{1}H NMR chemical shifts of **GS1** and **GS6** and compared the values with those of model enamines **10** and **11** (Figure 11). Enamine **10** shows optimal *N* lone pair–alkene π* interaction (dihedral angle 5-1-2-3 = 5°), while enamine **11** was constrained so that the *N* lone pair and alkene π* orbitals are orthogonal (dihedral angle 5-1-2-3 = 90°). The ^{1}H NMR results are shown in Figure 12.

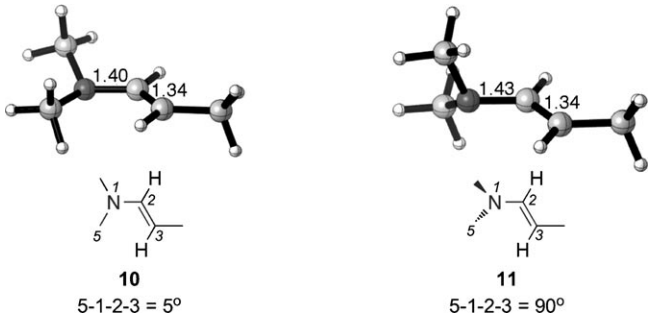

Figure 11. Conjugated (**10**) and nonconjugated (**11**) model enamines.

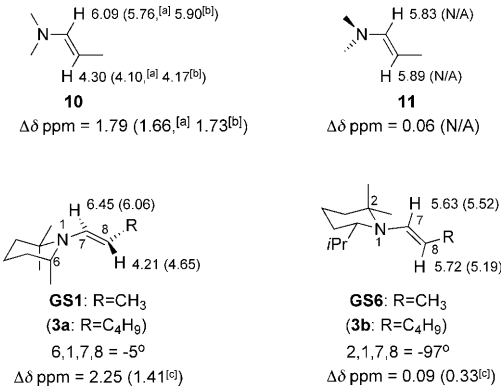

Figure 12. Calculated[d] and experimental ^{1}H NMR chemical shifts of olefinic protons. Experimental values are in parentheses. [a] [D_6]benzene, ref. [11]. [b] [D_8]THF, ref. [12]. [c] [D_6]benzene. [d] See Computational Methods.

The calculated ^{1}H NMR shifts of **10** are in good agreement with previously reported experimental values.[11,12] The computed shift difference of the olefinic protons of **10** is 1.79 ppm. When the alkene π* and *N* lone pair orbitals are orthogonal as in **11**, the difference decreases substantially to 0.06 ppm. The calculated chemical shift differences of the vinyl protons of **GS1** and **GS6** are 2.25 and 0.09 ppm, respectively. Although they do not mirror **10** and **11** or the experimental values exactly, they do follow the observed trend: conjugated enamines have a difference in chemical shift value of approximately 2 ppm, whereas non-conjugated enamines have a smaller chemical shift value, which is closer to 0 ppm.

Transition structures for alkylation of isopropyl enamine 3b*: While the lack of *N* lone pair–π* interaction (as indicated by the NMR data and in conformer **GS6**) might suggest that the isopropyl enamine **3b*** would not readily undergo alkylation,[5] experimentally it was found to undergo alkylation with both ethyl iodide and allyl bromide in 94:6 e.r. (Scheme 3).[4]

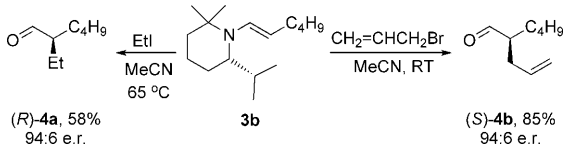

Scheme 3. Isopropyl enamine **3b** alkylation with ethyl iodide and allyl bromide.

Calculations support the experimentally observed preferential attack of ethyl iodide from the *Re* face (i.e., away from the now axial *i*Pr group) of enamine **3b***. Both *anti*-chair **TS9** and *anti*-twist **TS10** conformers of the transition state contribute (Figure 13).

Si-face alkylation of enamine **3b*** is significantly higher in energy (**TS11** and **TS12**, Figure 14); calculations predict a 96:4 e.r. ($\Delta\Delta G^{\ddagger} = 8.9$ kJ mol^{-1} at 65 °C) for ethyl iodide alkylation, which is in excellent agreement with the experimen-

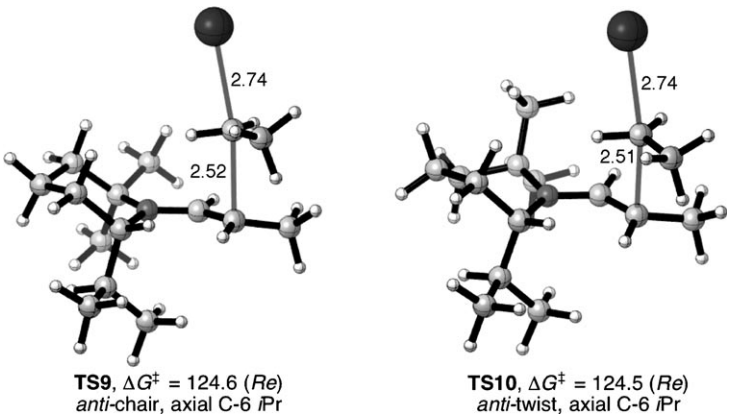

Figure 13. Transition states for *Re*-face alkylation of isopropyl enamine **3b*** with ethyl iodide.

© 2010 Wiley-VCH Verlag GmbH & Co. KGaA, Weinheim

tal observation that a bulky isopropyl group enhances asymmetric induction (94:6 e.r., $\Delta\Delta G^{\ddagger} = 7.7\ kJ\,mol^{-1}$ at 65 °C) compared with the methyl group (88:12 e.r.). The major contributor to the *Si*-face alkylation, **TS12**, has a twist conformation of the piperidine ring. This can be explained by the longer H–H distances in **TS12** compared to **TS11** as well as the larger stability of the ground-state twist (**GS9**) versus chair (**GS7**) conformation.

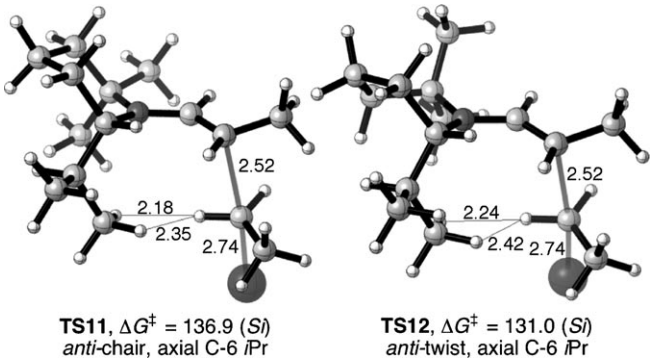

Figure 14. Transition states for *Si*-face alkylation of isopropyl enamine **3b*** with ethyl iodide.

Studies on the allylation of enamine **3b*** with allyl bromide were similarly carried out. The lowest energy *Re*- and *Si*-face transition structures are shown in Figure 15.[10] As expected, preferential attack of the electrophile takes place from the *Re*-face of enamine **3b***. The favored piperidine conformation for *Si*-face allylation is once again twist (**TS16**). The e.r. value was calculated to be >99:1 ($\Delta\Delta G^{\ddagger} = 14.4\ kJ\,mol^{-1}$ at 25 °C), compared with the 94:6 ratio ($\Delta\Delta G^{\ddagger} = 6.8\ kJ\,mol^{-1}$ at room temperature) found experimentally. Similar to the case of allylation of methyl enamine **3a***, the calculated selectivity is notably high. The hydrogen–bromide stabilization in the favored (*Re*) transition states **TS13** and **TS14** are up to 1.22 Å shorter than those of the corresponding ethyl iodide transition structures (**TS9** and **TS10**).[8] In the *Re*-face allylation of methyl enamine **3a***, **TS6** is not a major contributor to the major enantiomer of **4**, whereas both **TS13** and **TS14** contribute to the major enantiomer. Thus the overestimation of stereoselectivity is higher for isopropyl enamine **3b*** than for methyl enamine **3a***.

Conclusion

Density functional theory studies give a detailed picture of the transition states of these reactions and the factors controlling stereoselectivity. The computational modeling results parallel the experimental results, with $\Delta\Delta G^{\ddagger}$ error values ranging from 1.2–5.6 $kJ\,mol^{-1}$. Preferential attack of the electrophile proceeds from the less hindered *Re* face of enamines **3***. The theoretical calculations correctly predict that the ground-state conformation of enamine **3b*** is one

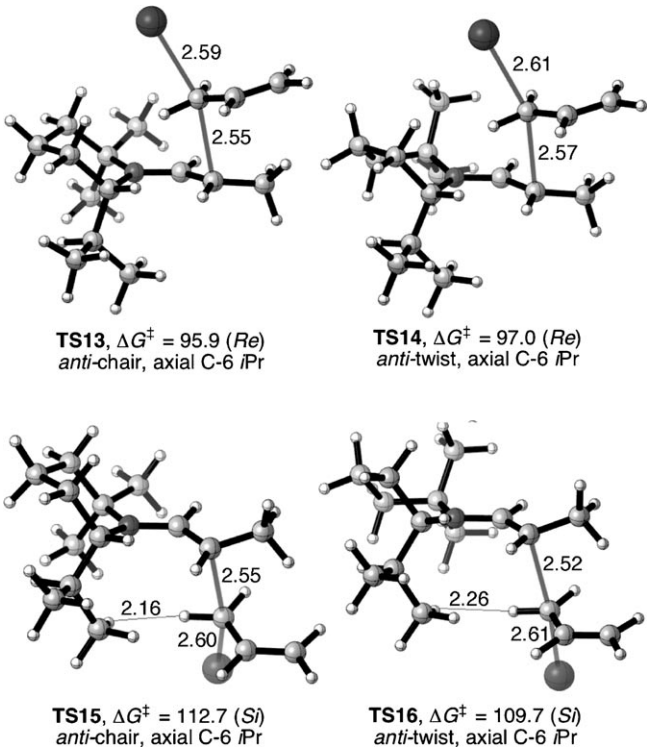

Figure 15. Lowest-energy transition states for *Re*- and *Si*-face alkylation of isopropyl enamine **3b*** with allyl bromide.

wherein the C-6 isopropyl is equatorial, but that the reactive conformer (where the C-6 isopropyl becomes axial) is attainable. The significant contribution of the twist conformer of isopropyl enamine **3b*** (**GS9**) to the disfavored alkylation transition states suggest that conformational biasing of the piperidine ring may lead to enhanced enantiomeric ratios. Investigations designed to improve the enantiomeric ratios of alkylated aldehydes **4** using alternative chiral enamines are now in progress.

Computational Methods

All ground-state (**GS**) and transition-state (**TS**) geometries were optimized in acetonitrile ($\varepsilon = 37.5$) using the CPCM model[13] with B3LYP[14] as implemented in Gaussian 03.[15] (It is also possible to calculate activation energies in solution and enzymes using the QM/MM methodology.)[16] The 6-31G(d)[17] basis set was applied to all atoms except for iodine, for which the LANL2DZ[18] basis set was used.[19] All stationary points were verified as minima or first-order saddle points by vibrational frequency analysis. NMR shifts were calculated using RB3LYP/6-311G+(2d,p)[20] and the GIAO[21] method on the B3LYP/6-31G(d) optimized geometries. The reported values are with respect to TMS, which was also calculated with the same method. Cartesian coordinates and energies of all reported structures are available in the Supporting Information.

Acknowledgements

We are grateful to the National Institute of General Medical Sciences, National Institutes of Health (GM 36700, K.N.H. and J.M.U.) and the

 © 2010 Wiley-VCH Verlag GmbH & Co. KGaA, Weinheim

Engineering and Physical Sciences Research Council (D.M.H. and N.S.K) for financial support of this work. Computations were performed on the UCLA Academic Technology Services (ATS) Hoffman2 cluster.

[1] For reviews, see: a) R. Göttlich in *Science of Synthesis: Houben–Weyl Methods of Molecular Transformations, Vol. 2* (Ed.: R. Brückner), Thieme, Stuttgart, **2006**, pp. 355–366; b) P. Melchiorre, *Angew. Chem.* **2009**, *121*, 1386; *Angew. Chem. Int. Ed.* **2009**, *48*, 1360–1363.

[2] a) N. Vignola, B. List, *J. Am. Chem. Soc.* **2004**, *126*, 450–451; b) A. Fu, B. List, W. Thiel, *J. Org. Chem.* **2006**, *71*, 320–326; c) See also: P. G. Cozzi, F. Benfatti, L. Zoli, *Angew. Chem.* **2009**, *121*, 1339–1342; *Angew. Chem. Int. Ed.* **2009**, *48*, 1313–1316.

[3] D. A. Nicewicz, D. W. C. MacMillan, *Science* **2008**, *322*, 77–80.

[4] D. M. Hodgson, N. S. Kaka, *Angew. Chem.* **2008**, *120*, 10106–10108; *Angew. Chem. Int. Ed.* **2008**, *47*, 9958–9960.

[5] a) D. M. Hodgson, C. D. Bray, N. D. Kindon, *J. Am. Chem. Soc.* **2004**, *126*, 6780–6781; b) D. M. Hodgson, C. D. Bray, N. D. Kindon, N. J. Reynolds, S. J. Coote, J. M. Um, K. N. Houk, *J. Org. Chem.* **2009**, *74*, 1019–1028.

[6] a) G. Stork, A. Brizzolara, H. Landesman, J. Szmuszkovicz, R. Terrell, *J. Am. Chem. Soc.* **1963**, *85*, 207–222; b) P. W. Hickmott, *Tetrahedron* **1982**, *38*, 1975–2050; c) *Enamines: Synthesis Structure and Reactions*, 2nd ed. (Ed.: A. G. Cook), Marcel Dekker, New York, **1988**; d) *The Chemistry of Enamines* (Ed.: Z. Rappoport), Wiley, New York, **1994**; e) T. Sammakia, J. A. Abramite, M. F. Sammons in *Science of Synthesis, Vol. 33* (Eds.: B. M. Trost, G. A. Molander), Thieme, Stuttgart, **2006**, pp. 405–441.

[7] We are aware of only two quantum mechanical studies on the stereochemistry of *C*-alkylation (S_N2) reactions of enamines: a) reference [2b]; b) A. Arrieta, F. P. Cossio, B. Lecea, *J. Org. Chem.* **1999**, *64*, 1831–1842. Reference [2b] describes the reactivity of pyrrolidine-based enamines, which are known to give different stereochemical outcomes than the six-membered analogues: c) P. H.-Y. Cheong, H. Zhang, R. Thayumanavan, F. Tanaka, K. N. Houk, C. F. Barbas III, *Org. Lett.* **2006**, *8*, 811–814. Reference [7b] describes acyclic enamines. For DFT studies of aldol and Mannich reactions by proline-type catalysts, see: d) A. Armstrong, Y. Bhonoah, A. J. P. White, *J. Org. Chem.* **2009**, *74*, 5041–5048; e) D. Seebach, U. Groselj, D. M. Badine, W. B. Schweizer, A. K. Beck, *Helv. Chim. Acta* **2008**, *91*, 1999–2034; f) A. Fu, H. Li, H. Si, S. Yuan, Y. Duan, *Tetrahedron: Asymmetry* **2008**, *19*, 2285–2292; g) A. Fu, H. Li, S. Yuan, H. Si, Y. Duan, *J. Org. Chem.* **2008**, *73*, 5264–5271; h) C. B. Shinisha, R. B. Sunoj, *Org. Biomol. Chem.* **2007**, *5*, 1287–1294; i) F. R. Clemente, K. N. Houk, *J. Am. Chem. Soc.* **2005**, *127*, 11294–11302.

[8] See the Supporting Information for a full analysis of the gas-phase and solution-phase geometries.

[9] a) J.-J. Delpuech in *Cyclic Organonitrogen Stereodynamics* (Eds.: J. B. Lambert, Y. Takeuchi), Wiley-VCH, Weinheim, **1992**, pp. 169–252; b) K. L. Brown, L. Damm, J. D. Dunitz, A. Eschenmoser, R. Hobi, C. Kratky, *Helv. Chim. Acta* **1978**, *61*, 3108–3135.

[10] See the Supporting Information for all conformers.

[11] J. B. Lambert, R. J. Nienhuis, *J. Am. Chem. Soc.* **1980**, *102*, 6659–6665.

[12] K. Tani, T. Yamagata, S. Akutagawa, H. Kumobayashi, T. Taketomi, H. Takaya, A. Miyashita, R. Noyori, S. Otsuka, *J. Am. Chem. Soc.* **1984**, *106*, 5208–5217.

[13] a) V. Barone, M. Cossi, *J. Phys. Chem. A* **1998**, *102*, 1995–2001; b) M. Cossi, N. Rega, G. Scalmani, V. Barone, *J. Comput. Chem.* **2003**, *24*, 669–681.

[14] a) A. D. Becke, *J. Chem. Phys.* **1993**, *98*, 5648–5652; b) A. D. Becke, *J. Chem. Phys.* **1993**, *98*, 1372–1377; c) C. Lee, W. Yang, R. G. Parr, *Phys. Rev. B* **1988**, *37*, 785–789.

[15] Gaussian 03, Revision C.02, M. J. Frisch, G. W. Trucks, H. B. Schlegel, G. E. Scuseria, M. A. Robb, J. R. Cheeseman, J. A. Montgomery, Jr., T. Vreven, K. N. Kudin, J. C. Burant, J. M. Millam, S. S. Iyengar, J. Tomasi, V. Barone, B. Mennucci, M. Cossi, G. Scalmani, N. Rega, G. A. Petersson, H. Nakatsuji, M. Hada, M. Ehara, K. Toyota, R. Fukuda, J. Hasegawa, M. Ishida, T. Nakajima, Y. Honda, O. Kitao, H. Nakai, M. Klene, X. Li, J. E. Knox, H. P. Hratchian, J. B. Cross, V. Bakken, C. Adamo, J. Jaramillo, R. Gomperts, R. E. Stratmann, O. Yazyev, A. J. Austin, R. Cammi, C. Pomelli, J. W. Ochterski, P. Y. Ayala, K. Morokuma, G. A. Voth, P. Salvador, J. J. Dannenberg, V. G. Zakrzewski, S. Dapprich, A. D. Daniels, M. C. Strain, O. Farkas, D. K. Malick, A. D. Rabuck, K. Raghavachari, J. B. Foresman, J. V. Ortiz, Q. Cui, A. G. Baboul, S. Clifford, J. Cioslowski, B. B. Stefanov, G. Liu, A. Liashenko, P. Piskorz, I. Komaromi, R. L. Martin, D. J. Fox, T. Keith, M. A. Al-Laham, C. Y. Peng, A. Nanayakkara, M. Challacombe, P. M. W. Gill, B. Johnson, W. Chen, M. W. Wong, C. Gonzalez, J. A. Pople, Gaussian, Inc., Wallingford CT, **2004**.

[16] a) O. Acevedo, W. L. Jorgensen, *Acc. Chem. Res.* **2009**, *42*, 724–733; b) O. Acevedo, W. L. Jorgensen, *J. Chem. Theory Comput.* **2007**, *3*, 1412–1419; c) O. Acevedo, W. L. Jorgensen, *J. Am. Chem. Soc.* **2006**, *128*, 6141–6146; d) O. Acevedo, W. L. Jorgensen, *Org. Lett.* **2004**, *6*, 2881–2884; e) A. Warshel in *Computer Modeling of Chemical Reactions in Enzymes and Solutions*, Wiley, New York, **1991**.

[17] a) R. Ditchfield, W. J. Hehre, J. A. Pople, *J. Chem. Phys.* **1971**, *54*, 724–728; b) W. J. Hehre, R. Ditchfield, J. A. Pople, *J. Chem. Phys.* **1972**, *56*, 2257–2261; c) P. C. Hariharan, J. A. Pople, *Theor. Chim. Acta* **1973**, *28*, 213–222.

[18] a) W. R. Wadt, P. J. Hay, *J. Chem. Phys.* **1985**, *82*, 284–298; b) M. W. Wong, P. M. W. Gill, R. H. Nobes, L. Radom, *J. Phys. Chem.* **1988**, *92*, 4875–4880; c) P. J. Hay, W. R. Wadt, *J. Chem. Phys.* **1985**, *82*, 270–283.

[19] B3LYP with the LANL2DZ basis set has been shown to effectively model the geometries and energies of iodo compounds. See: M. Tredwell, J. A. R. Luft, M. Schuler, K. Tenza, K. N. Houk, V. Gouverneur, *Angew. Chem.* **2007**, *120*, 363–366; *Angew. Chem. Int. Ed.* **2007**, *46*, 357–360, and references therein.

[20] a) A. D. McLean, G. S. Chandler, *J. Chem. Phys.* **1980**, *72*, 5639–5648; b) K. Raghavachari, J. S. Binkley, R. Seeger, J. A. Pople, *J. Chem. Phys.* **1980**, *72*, 650–654; c) M. J. Frisch, J. A. Pople, J. S. Binkley, *J. Chem. Phys.* **1984**, *80*, 3265–3269.

[21] K. Wolinski, J. F. Hilton, P. Pulay, *J. Am. Chem. Soc.* **1990**, *112*, 8251–8260.

Received: January 8, 2010
Published online: April 21, 2010

Please note: Minor changes have been made to this manuscript since its publication in *Chemistry–A European Journal* Early View. The Editor.

 © 2010 Wiley-VCH Verlag GmbH & Co. KGaA, Weinheim